Science of The Total Environment
Volume 722, 20 June 2020, 137875

Recent flood hazards in Kashmir put into context with millennium-long historical and tree-ring records

Juan Antonio Ballesteros Canovas [1,2,*], Tasaduq Koul [3], Ahmad Bashir [4], Jose Maria Bodoque del Pozo[5], Simon Allen [2], Sebastien Guillet [2], Irfan Rashid [4], Shabeer H. Alamgir [3]; Mutayib Shah [3]; M. Sultan Bhat [4], Akhtar Alam [6], Markus Stoffel [1,2,7]

1 Department of Earth Sciences, University of Geneva, Switzerland
2 Institute for Environmental Sciences, University of Geneva, Switzerland
3. Irrigation and Flood Control Department, Kashmir, India
4. University of Kashmir, Kashmir, India
5. Castilla La Mancha- University, Toledo, Spain
6. Institute for Risk and Disaster Reduction, University College London, UK.
7. Department F.-A. Forel for Environmental and Aquatic Sciences, University of Geneva, Switzerland

* Corresponding author: juan.ballesteros@unige.ch

Highlights

- Kashmir has recently suffered unprecedented flood disasters within the context of existing measurements
- These events have resulted in significant economic losses and fatalities
- Millennium-long historical and tree-ring flood records suggest that such extreme flood events are rather recurrent at centennial scale.
- The gained records contribute to a better flood-hazard assessment.
- The gained flood information is relevant given the special watershed management status encapsulated into the Indus Water Treaty.

ABSTRACT

In September 2014, the Kashmir valley (north-west India) experienced a massive flood causing significant economic losses and fatalities. This disaster underlined the high vulnerability of the local population and raised questions regarding the resilience of Kashmiris to future floods. Although the magnitude of the 2014 flood has been considered unprecedented within the context of existing measurements, we argue that the short flow series may lead to spurious misinterpretation of the probability of such extreme events. Here we use a millennium-long record of past floods in Kashmir based on historical and tree-ring records to assess the probability of 2014-like flood events in the region. Our flood chronology (635 CE –nowadays) provides key insights into the recurrence of flood disasters and propels understanding of flood variability in this region over the last millennium, showing enhanced activity during the Little Ice Age. We find that high-impact floods have frequently disrupted the Kashmir valley in the past. Thus, the inclusion of historical records reveals large flood

hazard levels in the region. The newly gained information also underlines the critical need to take immediate action in the region, so as to reduce the exposure of local populations and to increase their resilience, despite existing constraints in watershed management related to the Indus Water Treaty.

Keywords: flood, historical records, tree rings, Kashmir, Jhelum River, Indus Water Treaty

1. Introduction

In September 2014, the north-west of India and northeast Pakistan experienced incessant rains, which were particularly intense in the mountain region of Jammu and Kashmir (India). Massive floods and debris flows caused catastrophic damage in populated areas located along the main watercourses (Kumar and Acharya, 2016). The situation was especially dramatic in the Kashmir valley, where the Jhelum River flooded most of the inhabited land and crop fields, covering a surface of almost 853 km^2 (Romshoo et al., 2018). As a result of the 2014 flood, thousands of structures – mostly residential houses – in the main cities of the Kashmir valley were damaged (Farooq 2014). Key infrastructures such as hospitals, water and energy supply systems, communication lines, government establishments and cultural heritage sites were seriously affected. The situation resulted in an emergency with more than one hundred fatalities and thousands of families affected, as well as economic losses in the order of US$ 16 billion (Venugopal and Yasir, 2017). This extreme flood event required military rescue efforts (Tabish and Nabiac, 2015) and resulted in enhanced geopolitical tensions in the region that continue to the present day (Venugopal and Yasir, 2017).

The causes of this extreme event were attributed to the advection of moisture from the Arabian Sea as a result of the interaction between the westward-moving monsoon and the eastward-moving deep trough at mid-latitudes (Ray et al., 2015). In addition, the specific catchment characteristics of the Jhelum River – in particular the bowl-shaped topography of the valley – and land degradation over the last decades played an important role in the evolution of the flood event (Meraj et al., 2015; Figure 1). The magnitude of the flood was considered unprecedented, because it represented the largest discharge contained in systematic records (Farooq, 2014). Understanding the occurrence of such extreme floods is crucial when it comes to the implementation of Disaster Risk Reduction (DRR) strategies, as they can contribute to better preparedness and coping capacities, and as they can increase resilience of inhabitants against future flood disaster. The design and implementation of DRR activities seem highly relevant in Kashmir due to the extremely high vulnerability of the ever-growing population on the floodplains (population increase: 26% between 2001 and 2011 (Census of India, 2011), and multiplied by 10 since late 19th century (Digby 1890). This strong demographic increase has also resulted in increased exposure of infrastructures on the floodplains (Malik and Bhat, 2014).

Furthermore, the Kashmir valley represents a paradigmatic case in terms of water governance because watershed management is constrained by the Indus Water Treaty (IWT), signed in 1960 between India and Pakistan. The IWT states that the management of the Jhelum River belongs to Pakistan, even in the case of its tributaries within Indian territory. Although the IWT was a success in terms of solving legal issues related to water sharing between two countries, this special status also renders flood risk management highly challenging. Indeed, the implementation of structural measures (such as flood storage structures) requires the approval of both countries (IWT, 1960). The situation in the region may be aggravated in the near future given that climate change may result in increased precipitation through changes in monsoon activity (Gosain et al., 2006, Attri and Tyagi, 2010) and/or the advection of moisture from the Arabian Sea (Murakami et al., 2017).

Catastrophic floods such as the one that hit Kashmir in September 2014 are rare, i.e. are characterized by long recurrence intervals, which means that instrumental series are often too short to record several extreme events (Baker, 2008; Benito et al., 2015; Wilhelm et al., 2019). To study patterns of occurrence and to credibly estimate flood risk for the Jhelum River, it is critical to use information gathered over centennial and even millennial time scales. Here, we draw on a database of systematic records starting in 635 CE, tree-ring records of floods and historical archives, with the aim to develop a millennium-long record of extreme floods in the Kashmir valley. This unique record allows us to place the 2014 flood into context, and to provide a robust basis for the design and provision of more effective protective measures against future flood events in Kashmir.

2. METHODS

2.1. Study site description

The Kashmir valley is located in the north-west of the Indian Himalayan arc at the border with Pakistan (Figure 1). The valley is drained by the axial Jhelum River and has a length of 150 km from southeast to northwest, and a width of ~40 km from southwest to northeast, with an area of ~13,530 km^2. The length of the Jhelum up to the natural outlet of the Kashmir valley located at Baramulla is about 240 km, defining an average slope of 0.0001 m/m. The mild slope of the main river favours the formation of a meandering floodplain, where the population has established historically. The typical geomorphic setup of the Jhelum basin (Kashmir Valley) with its heterogeneous lithology, complex topography and varying hydrological conditions makes the basin susceptible to floods. The Jhelum basin is an inter-montane basin lying between the Pirpanjal mountain range along the W-E flank and the Great Himalayan mountain ranges along the N-E flank. Geologically, the Kashmir valley hosts two geological formations, the Panjal Volcanic Complex and Triassic limestones overlying Archean sediments. The rise of the Pir Panjal Range impounded the primeval drainage resulting in the formation of a huge lake inundating most of the plains of the Kashmir valley (Rashid et al., 2007; Rather et al., 2016). Changes in drainage were triggered by the uplift of the Pir Panjal Range, which sparked a sequence of interrelated tectonic, climatic and erosional processes that shaped the present geomorphic setup of the Jhelum River basin (Burbank and Johnson et al., 1983). Wular Lake is located in the northwest of the Kashmir valley, and is considered one of the largest freshwater lakes in India, with an important role in laminating floods (Romshoo et al., 2018). The Kashmir valley is affected by the southwest monsoon and extratropical disturbances (Das et al., 2002; Kalsi, 1980) originating from the Mediterranean and Caspian Seas. In winter, extratropical disturbances result in abundant snowfall, whereas monsoonal rains normally occur in summer. Average annual air temperature in Srinagar is 13.6 °C, with July (24.6°C on average) being the hottest month and January (1.5°C on average) the coldest month of the year. Annual rainfall averages 693 mm at Srinagar. Kashmir has a temperate climate according to Köppen's classification (Köppen 1936). Over the last decades, the Kashmir valley has suffered intense forest degradation and has lost ~0.45% of its forest cover every year between 1930 and 2013 (Wani et al., 2016; Rather et al., 2016; Reddy et al., 2016). Most of the forest degradation has taken place in the Pir Panjal mountain range lying towards the W-E flank of the Kashmir valley (Figure S7). During the same period, settlements increased by ~400%, not only contributing towards further forest degradation but also encroaching upon wetland areas within the floodplain of the Jhelum River.

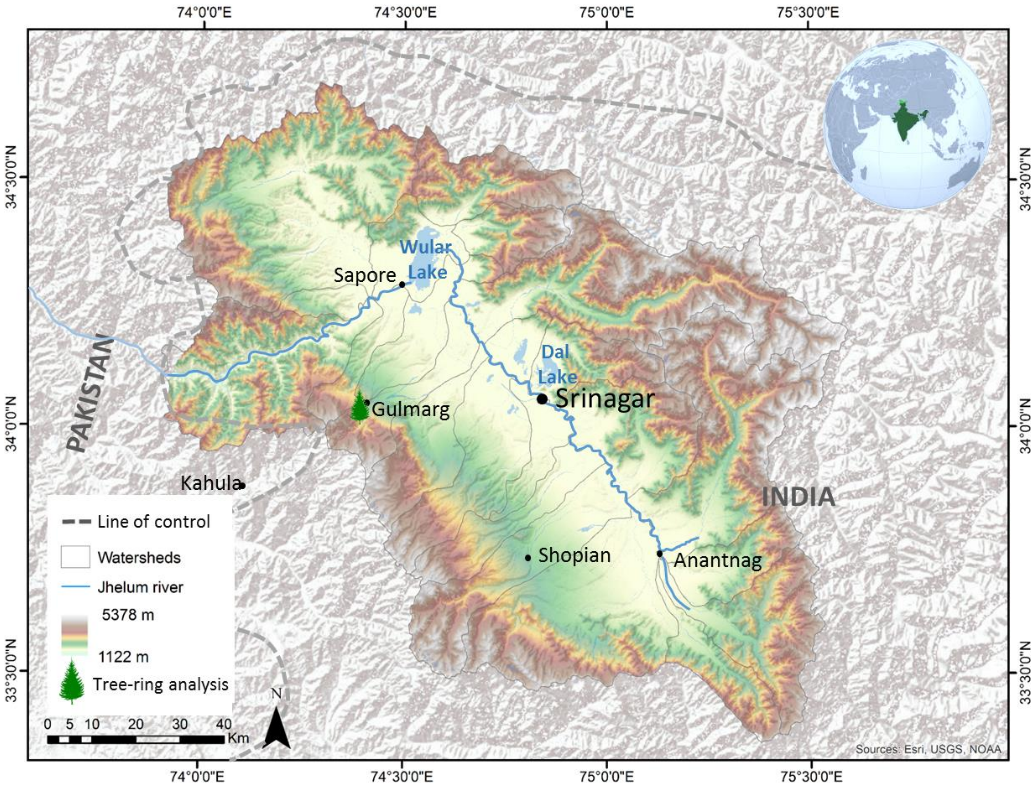

Figure 1. The Kashmir valley is located in the northwestern part of India, in the state of Jammu and Kashmir. Historical sources refers to the flood activity of the Jhelum river, while the tree-ring flood reconstruction is based in the mountain tributary located at Gumarg.

2.2. Analysis of historical sources

To reconstruct the floods of the Jhelum River over the past millennium, we investigated more than thirty historical sources. Our analysis relied mostly on contemporary records (see Figure S1). We also complemented our survey with secondary sources. Thus, seventeen records investigated in this study are primary sources, whereas eleven are secondary sources (Figure S1). Most of the sources surveyed are chronicles and travel accounts. These sources were mostly written in Persian (most of them were, however, translated to English), Sanskrit or, in the case of travellers' accounts, English. For the most recent period (1956-nowdays), we used the systemic record of the Irrigation and Flood Control Department (IFCD) (www.ifckashmir.com). The reliability of each account was assessed with a rating scale following the methodology described in Barriendos et al. (2003), where: **A** are eyewitness or contemporary chronicles with a reliable chronology; **B**: eyewitness or contemporary sources, but with some chronological uncertainty or neither eyewitness nor contemporary but has a reliable chronology and/or accurately conveys the information from earlier works; **C:** eyewitness or contemporary but with evidence of errors or fabrications, or neither eyewitness nor contemporary and with an unreliable chronology; and where **D:** are neither eyewitness nor contemporary and with evidence of errors or fabrication. To assess the magnitude of past flood events, we followed the approach defined by Barriendos et al. (2003). Each flood event was classified as ordinary, extraordinary, and catastrophic based on the descriptions found in historical accounts (i.e. flood effect on the river bed and surrounding areas, water level, damage to infrastructure). For each category, flood discharge was modelled using calibrated hydraulic models based on the thresholds described in the hydraulic modelling section (see below).

2.3. Tree-ring-based flood reconstruction

Tree-ring records were used to reconstruct past flood events in the study area. Trees presenting obvious evidence of flood events (i.e. scars oriented according to the flow direction, tilted trees) were preferentially targeted. Samples from 58 disturbed trees were prepared following standard dendrochronological procedures (Ballesteros-Canovas et al., 2015). Cores were mounted on wooden sticks and then polished with sandpaper. Tree rings were counted and analyzed using a LINTAB-5 positioning table connected to a Leica stereomicroscope. Individual tree-ring series were cross-dated using a local reference chronology – obtained after sampling 15 undisturbed trees near the study site - so as to correct our series for possibly missing rings. In a second step, all cores were visually inspected under a stereomicroscope to identify growth disturbances (GDs) induced by floods such as: (i) injuries and callus tissues; (ii) tangential rows of traumatic resin ducts (TRDs); (iii) reaction wood; (iv) abrupt growth. Finally we developed the flood reconstruction using the weighted index factor (W_{it}) described in Ballesteros-Canovas et al. (2015, see also Figure S8). The W_{it} gives a weight to each GDs based on its intensity and based on the number of trees impacted for a given year.

2.4. Hydraulic modelling

We used the HEC RAS hydraulic model to estimate the magnitude of historical floods. To this end, we used the bathymetry information obtained during field survey by the IFCD. Floodplains were then added based on the 8-m resolution DEM retrieved from the High Mountain Asia Dataset available at the NASA National Snow and Ice Data Center Distributed Active Archive Center (NSIDC DAAC) https://nsidc.org/data/highmountainasia. In total, the model was set up with 43 cross section in the surrounding of the Munshibagh flow gauge station (34,07°; 74,82°). For each cross-section, we used contraction and expansion coefficients according to a gradual transition flow (0,1 and 0,3, respectively). The rating curve of the gauge station was used to calibrate the roughness parameter in the model (Figure S9). The calibration process reported Manning's values ranked from 0,1 to 0,5 in floodplains and 0,03 to 0,065 in the channels for low-to-intense recorded flood magnitudes, respectively (Figure S4). The model was run considering steady flow condition.

Once the model was set up, we considering the roughness-magnitude relation from the calibration process to estimate the 2014 flood magnitude based on the maximum height recorded at Munshibagh (Figure S6). Moreover, we used the model to estimate the flood magnitude associated to thresholds of past events according to the following categories (Figure S5): (i) ordinary floods, i.e. events slightly over the bankfull flooding level; (ii) extraordinary floods, i.e. events over flooding the bankfull capacity with moderate capacity to impact populations, but mostly agriculture lands (<1.5 m water depth); and (ii) catastrophic floods, i.e. floods with the capacity to cause severe damage or complete destruction to the infrastructures or close to the river (> 1.5 water depth; Figure S5).

2.5. Flood return period estimation

Before conducting the flood-frequency analysis (FFA), an initial exploratory data analysis was undertaken. The degree of linear dependence among successive observations was tested using a correlogram as a visual approach to detect the existence of serial correlation (Salas, 1993). Statistical methods were used to merge the reconstructed flood discharges with the systematic records. In a first step, stationarity of the reconstruction was checked using Lang's test (Lang et al., 1999). This test assumes flood records are distributed following a homogenous Poisson process at the 95% tolerance interval. Stationary flood series are defined as those remaining within the 95% tolerance interval (Naulet et al., 2005).

Here, we employ the FFA approach proposed by the U.S. National Flood Frequency Guidelines Bulletin 17C (England et al., 2018). These guidelines are based on the Pearson type III distribution with logarithmic transformation of flow data (England et al., 2003). For the estimation of the Pearson type III distribution parameters, EMA, a generalized method of moments procedure was implemented (Cohn et al., 2001, 1997). Further, we used Multiple Grubbs-Beck statistic to identify multiple potentially influential low flows, or PILFs (Cohn et al., 2013).

Moments estimation of the log-Pearson III distribution was based on the representation of flow data by intervals (i.e. for a particular year Y, the flow Q was represented as $Q_{Y,lower}$ and $Q_{Y,upper}$) and perception thresholds (Table 1). In the case of systematic data, we assumed that flow is known accurately, so $Q_{Y,lower} = Q_{Y,upper}$ = QY. By contrast, PILFs were handled as censored data (Cohen, 1991), i.e., $Q_{Y,lower} = 0$; $Q_{Y,\ upper} = Q_{l}$. For non-systematic data, three different approaches were used for data representation, namely (i) interval (Cohn et al., 1997), i.e., floods of known magnitude within a range or interval; (ii) binomial-censored (Stedinger and Cohn, 1986), i.e., floods in which there is certainty that a given flow was exceeded, but its real magnitude is unknown; and (iii) points, i.e., $Q_{Y,lower} = Q_{Y,upper}$ = QY. EMA also required the determination of perception thresholds to estimate confidence intervals. They were calculated on the basis of both the historical and tree-ring based flood reconstructions. Prior to the period of systematic data, perception thresholds represent the potential range of flows ($T_{Y,lower}$, $T_{Y,upper}$) that would have left their footprint in case that flooding occurred. For non-systematic data, the $T_{Y,lower}$ was defined as the lowest flow estimated from historical records, whereas $T_{Y,upper}$ was equalled infinity. For systematic data, $T_{Y,lower}$ was preliminarily represented as the smallest flood flow recorded and characterized by baseflow measurement, whereas $T_{Y,upper}$ was assumed to be infinite. In the case of gaps in the records (i.e. broken records), both thresholds were set to infinity. Maximum annual peak discharge and water stages were used to determine a rating curve at this site (Figure S9).

3. Results and discussion

3.1. Historical and tree-ring based flood reconstruction in Kashmir

We complemented the existing systematic flow measurements with historical and tree-ring based flood records covering the past millennium in the Kashmir valley. The historical flood reconstruction in Kashmir benefits from the existence of twenty-eight primary and secondary sources, as well as documents from the local authorities (Table S1; Figure S1).

Historical records testify the occurrence of forty-eight flood events from the early seventh century to 1950 CE (Figure 2, Figure 3, Table S1). Considering the entire period from 635 to 2015 CE, the average rate of extreme flooding at Jhelum River is 0,038 floods yr^{-1}. Besides, tree-ring based flood records also point to the regular occurrence of additional, torrential floods at Gulmarg over the last centuries, with 11 floods dated between 1880 and 2018, defining an average occurrence rate of 0,08 floods yr^{-1}.

We identified evidence for 64 historical floods containing information about the causes, mechanisms, and impacts of past events in the Kashmir valley. The earliest accounts in the Common Era (CE) describe large floods during the reign of the Raja Durlab Vardhana (617–635 CE), and later during the reign of Lalitadatiya (724-761 CE). Similarly, historical accounts describe a flood in 879 CE affecting large parts of the Kashmir valley. This event was apparently induced by a co-seismic landslide and the subsequent blocking of the river, thus also pointing to the co-existence of complex triggering mechanisms and compounded events in the region.

Until the 16th century, historical records describe the existence of recurrent, yet intense floods with dissimilar impacts upon the Kashmiri society (i.e. 917-918; 1013; 1063-1089; 1099; 1128; 1135; 1342-1354; 1354-1373; and 1462 CE, see supplementary data). Specifically, the 1462 flood largely affected the Kashmiri population, as described in the *Rajatarangini of Jonaraja* (1587): "*a dust rain descending on tooth from the sky, and indicating a famine. Not long after, heavy clouds with the rainbow, and peals of loud thunder, terrified the people,* *even like enemies with their arrows. Bubbles appeared on the water, beaten by the rain, and seemed like the heads of snake's intent on destroying the crops; and the clouds, which raised the bubbles threatened to destroy all that would grow*". Between the 16th and 18th centuries, the number of historical accounts increases, as are reports on recurrent flood occurrences in 1514-1516; 1541; 1569; 1576; 1577; 1585-1589; 1604; 1640-42; 1643; 1651; 1662; 1678; 1683; 1706; 1711; 1723-4; 1729-1731; 1733-4; 1735; 1745; 1747; 1770 and 1787-8 CE, always with similar impacts on the society. In the 19th century, 14 floods have been documented that affected crops and infrastructures causing famines and the outburst of diseases like cholera (see Table S1). The flood in 1893 was described in detail in the travel accounts of Walter Lawrence in 1895, stressing the combined role of long-lasting rainfall and snowmelt processes in triggering the floods. During the 20th century, several floods have been recorded in different sources, and have even been represented in artistic work. In 1903, a large flood affected the main cities of the valley, as is reflected in the traditional song *Sailab Nama* composed by Hakim Habibullah, and also in the poem entitled "*The Flaying Cranes*" by Rabindranath Tagore in 1915. Moderate floods occurred then in the first half of the past century, namely in 1900; 1902; 1903; 1905, 1909, 1912, 1928, 1950, and 1957 CE. The flood registered in 1959 (1302 m^3/s) by the gauge station located at Srinagar was disastrous, with more than one million people and a thousand villages affected. Since then, major floods (>90th percentile) were recorded at Munshibagh (Jhelum river) in 1966 (1003 m^3/s), 1973 (1223 m^3/s), and 1976 (970 m^3/s). In 2014, the gauge station was overflooded; however, the maximum height allowed estimation of the flow gauge based on a calibrated hydraulic model to 2200 m^3/s. Later, minor flood-like situations arose in June 2015 as well as in June 2018 but did not cause significant damage in the valley. Likewise, tree-ring records points to the existence of 11 torrential floods in 1881, 1893, 1925, 1961, 1962, 1966, 1973, 1985, 1988, 2000, 2002 and 2010 CE. Some of these events (i.e. 1966, 1973, 1988 and 2010) were recorded downstream by the flow gauge station at Feroz pora river.

The sources we investigated also reveal strong socio-economic impacts induced by major past floods. Archives report in detail how excessive rainfall and long-lasting inundations of the Jhelum floodplain not only resulted in loss of human lives and damage to property, but also in the inundation of agricultural fields and the destruction of crops (Figure 2-C; Table S1). The subsequent harvest failures often led to severe price inflation and, in the most critical instances, to severe food crises and famines as evidenced in the *Rajatarangini* (*River of Kings*) chronicle written by Kalhanas in the 12th century: *In 917-918 CE, human skeletons and bones were spread in all directions in the Valley making it seems like a great burial-ground due to famines periods. In this year, rice crops were destroyed due to a flood causing famines as well*. Out of the 48 major floods identified, 26 have caused famines (see Table S1). However, it would be inaccurate to assume that communities were helpless in the face of environmental hazards. For instance, the *Rajatarangini* of Kalhana reports that in the 8th century, King Lalitadatiya (782-794 CE) decided to move the capital city to safer ground after a catastrophic flood that severely affected the main city: *During the reign of King Lalitadatiya, the main city was submerged. The King shifted the capital to Letapore, 22 km to the south. Most of the houses in the town were also destroyed*. Besides these accounts, we also exhumed reports enumerating the multiple measures that were implemented over the past centuries to mitigate and prevent flood hazards in the valley. This includes the digging of a channel near Khadanyar to increase the flow capacity of Jhelum River at the valley outlet after the occurrence of a major flood in 879 CE (Rajatarangini of Kalhanas, 1149). Repeat hydraulic works included the artificial canalization of the river and the construction of flood channels and continued from the 9th to the early 20th century (after the 1903 flood event, but also include measures taken after the 2014 flood (Table S1). However, the efficiency of protection works and mitigation appears to have been rather limited as they did not prevent the floods of Jhelum river from causing death and destruction on the floodplains. Yet, they illustrate that attitudes of communities and authorities toward risk were neither passive nor static, even in the distant past (Table S1).

The investigated sources also provide a picture of the evolution of the wetlands in Kashmir over the centuries (Figure 2-E; Table S2; Figure S2). According to historical accounts, the size of Wular lake reached its maximum extension during the 18^{th} and 19^{th} centuries (up to ~200 km^2). By contrast, the minimum extension of the lake occurred during the 6-7^{th} centuries, 16-17^{th} centuries, and nowadays during the late 20^{th} century (lake extension between 55 and 90 km^2). Thus, the freshwater surface of Wular lake has been reduced significantly over the last century due to siltation processes, from 89 km^2 in 1911 to 9.5 km^2 nowadays (Romshoo et al., 2018). The siltation process has contributed to reduce the capacity of the lake to laminate flood discharge and increase the effect of backwater effects during extreme events (Romshoo et al., 2018).

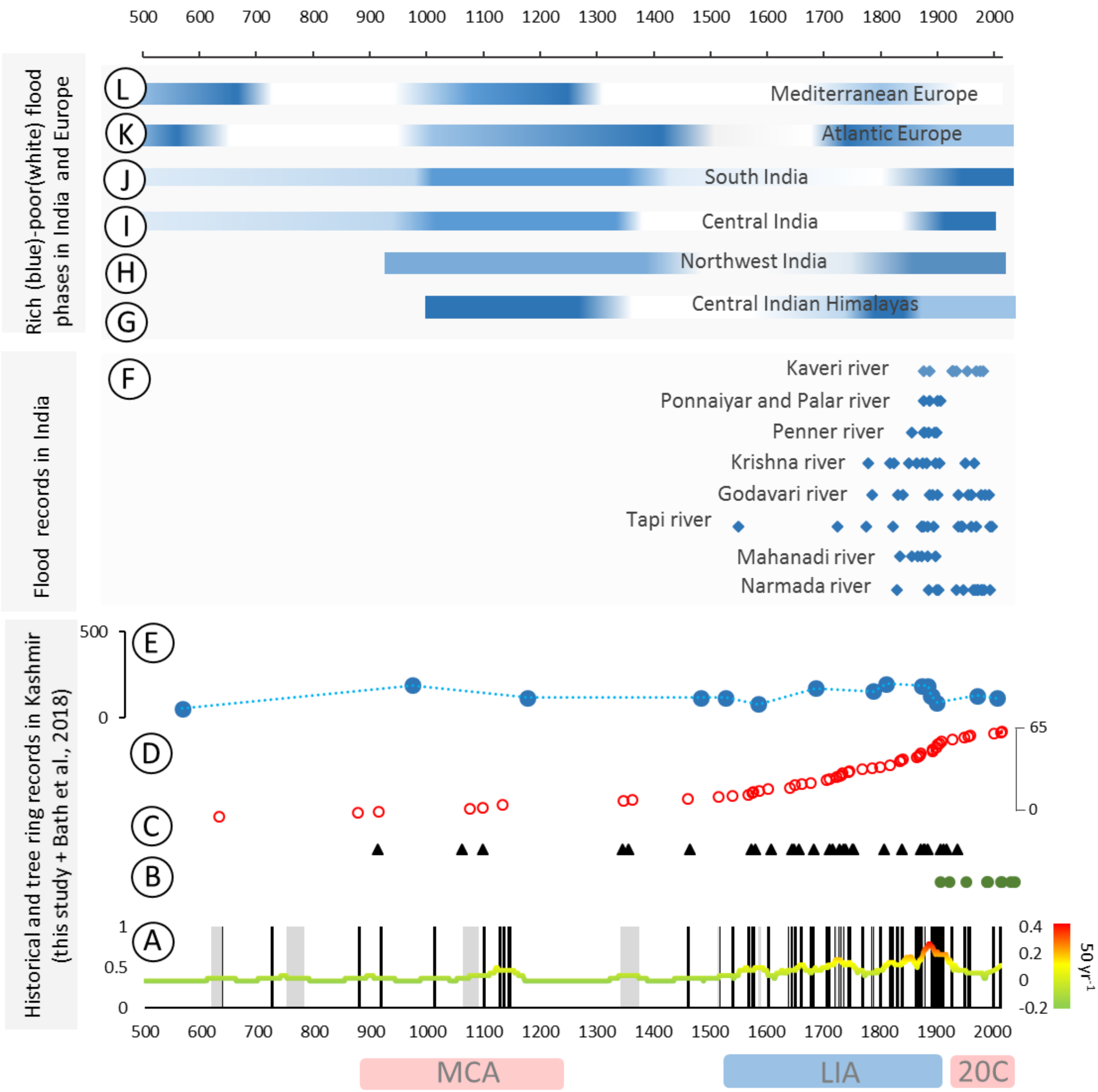

Figure 2. Compilation of the historical flood information provided in this study. Fig2-A) Chronology of historical flood records for the Jhelum River detected based on primary and secondary sources (Table S1) in Kashmir, showing the different warm/cold periods of the Medieval Climate anomaly – MCA, the Little Ice Age – LIA (Kaul, 1990; Rowan, 2017) and the ongoing warming. Fig 2-B) Tree-ring flood records identified at the tributary of the Jhelum River at Gulmag. Fig2-C) Years with historical records linking famines due to flooding. Fig 2-D) Flood accumulation at Jhelum River. Fig 2-E) Evolution of the Wular lake size based on historical accounts (Table S2) and recent remote sensing (2); Fig 2-F)

Historical floods in different Indian rivers (Kale, 1997a); Fig 2-G-L) Dissimilar high (blue) and low (white) flood phases in different locations, including Atlantic and Mediterranean regions (F: Wasson et al., 2013; G: Kale et al., 2000; H: Kale, 1997; I: Thmas et al., 2007; J and K: Benito et al., 2015).

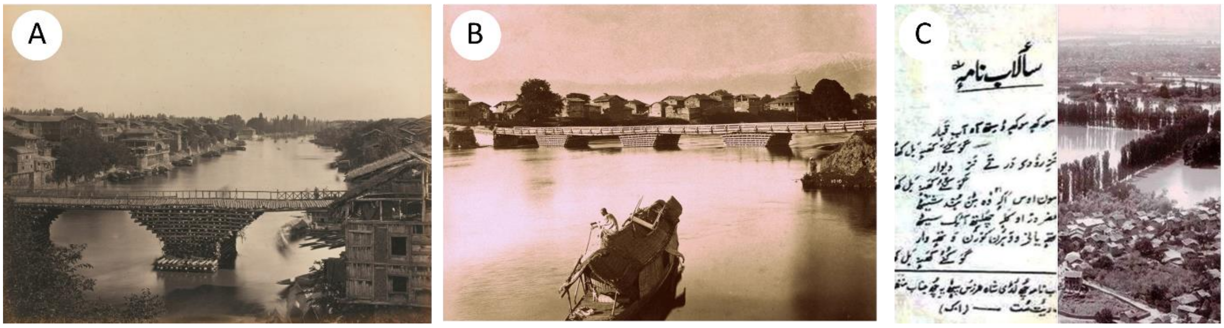

Figure 3. Picture of the bridges over Jhelum River at Srinagar under non-flood conditions (Fig.3-A) and during the flood of 1893 (Fig.3-B). Fig.3-C traditional song "Sailab Nama" composed by Hakim Habibullah and picture of the flood in 1903. Sailab Nama: "Slowly, slowly horrible waters came from Khanabal to Khadenyaar, it was a sheet of water and everything got destroyed".

3.2. Contextualizing floods and climate variability

Comparison of the Jhelum River records is in line with existing paleoflood information from the northwestern Himalayas (Wasson et al., 2013) over the last five centuries. Our flood records also agree with reconstructed periods with wetter climatic conditions in the region, based on tree-ring records (Treydte et al., 2006). The Jhelum River flood chronology also resembles flood activity in the Mediterranean region over the last centuries (Benito et al., 2015), with an increase in flood activity at the end of the Spörer (~ 1460–1550; Eddy, 1976) and Maunder (~1645-1715; Eddy, 1976; Shindell et al., 2001) Minima (see Figure 2). We also observe increased flood activity between the end of the Little Ice Age (LIA) and the late 19^{th}

century. However, our flood reconstruction differs from others developed in the Indian Peninsula where authors suggest an increase of extreme floods over the last decades in comparison to paleoflood records (Ely et al, 1996), especially during the LIA (Kale and Baker, 2006; Kale and Hire, 2007). The increase in flood records in our reconstruction during the 18th century and late 19th century is in line with those observed in the upper Ganga catchment (central Indian Himalayas; Wasson et al., 2013), and has been explained as the result of enhanced wind speeds over the Arabian Sea. Such an increase in wind speed over the Arabian Sea is known to favour the advection of moist air masses over northwest India, causing intense rainfall (Murakami et al., 2017). Noteworthy, this mechanism was also involved in the triggering of the 2014 flood event in Kashmir (Ray et al., 2015), and likewise at the origin of the 2010 Pakistan floods (Webster et al., 2011).

3.3. Revisiting the likelihood of extreme floods in Kashmir

Lang's test provides evidence for the presence of stationarity in historical flood records between 1500 CE and today; and from 1880 CE and today for torrential floods reconstructed from tree-ring data (Figure 4-A; Figure S3). The Mann-Kendall test (τ = 0,016; p-value = 0,857 and Theil slope = 0,288 m^{3}sec^{-1}) is also supporting the assumption that the systematic time series does neither contain an increasing or decreasing trend over time. Consequently, the flood frequency analysis for the Jhelum River and historical accounts was restricted to this period. Based on the calibrated hydraulic model (Figure S4, S5 and S6), we estimated the magnitude of 39 past floods, which were include as censored values, upper and lower thresholds and a range of values in Figure 4-B. Hydraulic model results reported ordinary floods (i.e. slightly over the bankfull level) with an estimated peak discharge of up to 600 m^3/s; extraordinary floods (i.e. (<1,5 m water depth) with an estimated peak discharge between 600 and 1200 m^3/s; and catastrophic floods (> 1,5 water depth) with a peak discharge exceeding 1200 m^3/s. In addition, we estimated peak discharge of the 2014 as being ~2200 m^3/s for the reach under investigation (Figure S6; for details see Methods).

Peak annual flows were not significantly autocorrelated, indicating that the estimated p-value is appropriate and not impacted by autocorrelation. The flood frequency assessment was carried out using Moments estimation (EMA) with the Multiple Grubbs-Beck statistic for the detection of PILFs. As shown in Fig. 4-C, there are 3 floods in the systematic record that exceed the historical threshold (1200 $m^3 s^{-1}$), namely in 1957 (1299 m^3 s^{-1}), 1959 (1266 m^3 s^{-1}) and 1962 (1973 m^3 s^{-1}). The implementation of the Multiple Grubbs-Beck statistic allowed the identification of 8 PILFs, with a threshold of 333 m^3 s^{-1} and with p-values comprised between 0,3869 and 0,0004. As a result, the 8 peak flows smaller than 333 m^3 s^{-1} were treated as censored data, so they were recoded to define flow intervals of ($Q_{Y,lower}$ = 0; $Q_{Y,\ upper}$ = 333 m^3 s^{-1}). PILFs also had the impact of altering the lower bound of the perception threshold for the systematic data period from 1955 to 2015. Thus, the perception threshold shifted from ($T_{Y,lower}$ =0) to ($T_{Y,lower}$ =333). For historical binomial-censored data, the lower limit of the perception threshold was set at $T_{Y,lower}$ = 1200 m^3 s^{-1}, whereas for interval (historical) data, $T_{Y,lower}$ was fixed at 600 m^3 s^{-1}. The flood frequency results (Fig. 4-C; Table 2) indicate that the log-Pearson type III model fits most data reasonably well, including the bulk of large floods, but underestimates the magnitude of the biggest flood (2014 -2200 m^3 s^{-1}). As such, the annual exceedance probability of a possible future flood similar to the one in 2014 will rank between ~ 0,01 and 0,005, depending on whether or not with regional skew in the dataset is considered in the assessment (Table 2).

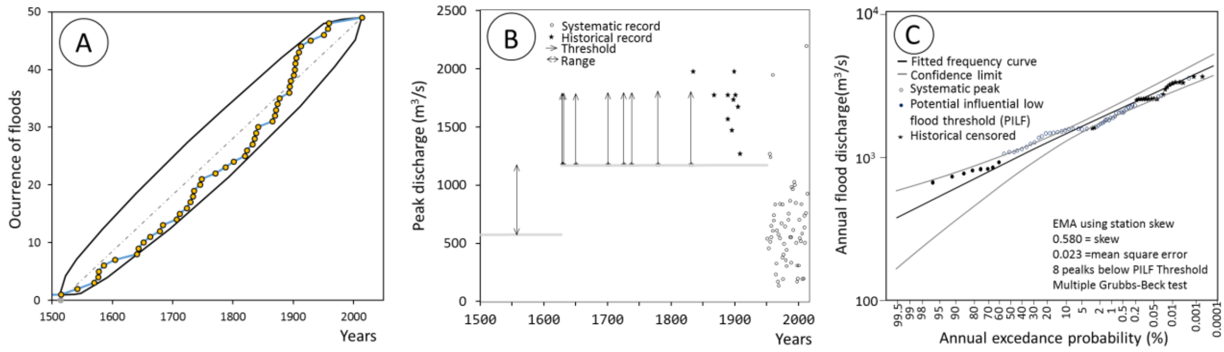

Figure 4. A) Lang's test for flood accumulation since beginning of 16th century. B) Composite of reconstructed (historical) and systematic peak discharge values for past floods in the Jhelum River at Srinagar. C) Flood frequency assessment with and without historical records.

Table 1. Generalized data representation of peak-flows interval and perception thresholds (England et al., 2018)

Data source	Data type	Flow interval	Perception threshold
Gage	Point	$Q_{Y,\,lower} = Q_Y$ $Q_{Y,\,upper} = Q_Y$	$T_{Y,\,lower} = 0$ $T_{Y,\,upper} = \infty$
Historical	Interval	$Q_{Y,\,lower} > Q_h$ $Q_{Y,\,upper}$	$T_{Y,\,lower} = Q_h$ $T_{Y,\,upper} = \infty$
Historical	Binomial	$Q_{Y,\,lower} \geq Q_h$ $Q_{Y,\,upper} = \infty$	$T_{Y,\,lower} = Q_h$ $T_{Y,\,upper} = \infty$
Historical	Point	$Q_{Y,\,lower} = Q_Y$ $Q_{Y,\,upper} = Q_Y$	$T_{Y,\,lower} = Q_h$ $T_{Y,\,upper} = \infty$
PILFs	Censored	$Q_{Y,\,lower} = 0$ $Q_{Y,\,upper} = Q_l$	$T_{Y,\,lower} = Q_l$ $T_{Y,\,upper} = \infty$

Table 2. Peak flow quantiles in cubic meters per second based on FFA using EMA and Multiple Grubbs-Beck test. Variance of estimates are shown in log space

Annual exceedance probability	EMA estimate ($m^3 s^{-1}$), with regional Skew	EMA estimate ($m^3 s^{-1}$) without regional Skew	Variance of estimate	Lower 2,5% confidence limit ($m^3 s^{-1}$)	Upper 97,5% confidence limit ($m^3 s^{-1}$)
0,5	404,8	421,9	0,0011	309,7	450,3
0,2	706	684,5	0,0005	637,8	772,1
0,1	940,6	914,6	0,0005	851,2	1041
0,04	1274	1283	0,0008	1140	1458
0,02	1547	1622	0,001	1367	1824
0,01	1840	2026	0,0014	1600	2235
0,005	2155	2507	0,0019	1839	2699
0,002	2607	3285	0,0028	2162	3415

4. Implications for flood risk management in Kashmir

Results from the combined analysis of instrumental data with multi-proxy records support that Kashmir region is highly susceptible to extreme flood events. Thus, intense floods at Jhelum river occurred roughly four times per century (0,038 floods yr^{-1}) over the last millennium, while the torrential activity in tributaries mountains stream has been reported even higher (0,08 floods yr^{-1}) over the last century. Our assessment also suggests that the annual exceedance probability of 2014-like flood events may rank between ~ 0,01 and 0,005. In the next decades, the ever-increasing demographic pressure in Kashmir could increase the negative impacts of floods (Meraj et al., 2015). Thus, the likely strengthening of convergence in the western Himalayas of the moisture carrying wind from the Arabian Sea may favour deep convection phenomena and an intensification of monsoon activity over the Kashmir region (Murakami et al., 2017). Besides, climate models also point to a possible increase in extreme precipitation over the region (Turner and Annamalai, 2012; Jie et al., 2017 Rao et al., 2014; Palazzi et al., 2013), which could occur early in the spring season as a result of elevation-dependent warming (Pepin et al 2015), enhancing the possibility of rain-on-snow floods, similar to the extreme flood reported in 1893 (i.e. Lawrence 1895). Besides, the intensification of runoff is furthermore enhanced by progressing forest degradation in region (Wanni et al., 2016; Rather et al., 2016; Rashid et al., 2017), which has a clearly negative impact on the siltation of the lakes (wetlands) in the valley (Figure S 7 and Table S2), and consequently in their lamination capacity. Last, but not least, the new formed glacial lakes due to shrinking of glacier mass may increase the probability of glacier lake outburst floods (GLOFs) with disastrous consequences in the region (Govindha Raj et al., 2010).

The results of this study call for an immediate and very carefully thought implementation of proper management mechanisms in the region so as to limit further, and unbalanced, increases in exposure and vulnerability, but also to reduce future flood impacts in Kashmir. We argue that the information provided here is highly relevant, not only to raise awareness at institutional levels, but above all also for the design of new strategies aimed at improving the resilience of Kashmiris against extreme flood events. Given the complexity of Kashmir water management, as it is encapsulated in the Indus Water Treaty (IWT) (Rao, 2018), and the political sensitivity of the region, the impact of future extreme floods or the occurrence of more frequent, yet moderate floods will not only result in human disasters, but could also fuel geopolitical crises between both countries (Rao, 2018). A proper definition and implementation of solutions that can minimize the negative impacts of future floods in Kashmir in a sustainable and constructive manner by both countries is thus not only desirable, but a clear need for the immediate future.

Acknowledgment: This research has been funded through The State Secretariat for Education, Research and Innovation (SERI) and ZHAW as Leading House for the bilateral research collaboration between India and Switzerland.

Author contributions: JABC, TK, SHA, MShah, MS designed research. JABC, AB, GS, TK, IR, MSB, AA, SA contributed new reagents/analytic tools. JABC, AB analysed data. JABC lead writing. All contributed to write and review the paper.

Additional information: The authors declare no conflict of interest

REFERENCES

Allen, S.K., Ballesteros-Canovas, J., Randhawa, S.S., Singha, A.K., Huggel, C., Stoffel, M. 2018. Translating the concept of climate risk into an assessment framework to inform adaptation planning: Insights from a pilot study of flood risk in Himachal Pradesh, Northern India. *Environ Sci Poli* **87**: 1–10.

Attri, S.D., Tyagi, A 2010. *Climate profile of India. Environment Monitoring and Research Center*, India Meteorology Department: New Delhi, India.

Baker, V.R. 2008. Paleoflood hydrology: Origin, progress, prospects. *Geomorphology*, **101(1-2)**: 1-13.

Ballesteros-Cánovas, J.A., Stoffel, M., St George, S., Hirschboeck, K. 2015. A review of flood records from tree rings. *Prog. Phys. Geogr*, **39(6):** 794-816.

Barriendos, M., Cœur, D., Lang, M., Llasat, M.C., Naulet, R., Lemaître, D., Barrera, A 2003. Stationarity analysis of historical flood series in France and Spain (14th–20th centuries). *Nat. Hazards Earth Sys Sci*, *3(6)*: 583-592.

Benito, G., Brázdil, R., Herget, J., Machado, M.J. 2015. Quantitative historical hydrology in Europe. *Hydrol Earth Syst Sci*. **12(4)**.

Benito, G., Macklin, M.G., Panin, A., Rossato, S., Fontana A., et al., 2015. Recurring flood distribution patterns related to short-term Holocene climatic variability. *Sci Rep* **5**: 16398.

Burbank, D.W., Johnson, G.D. 1983. The late Cenozoic chronologic and stratigraphic development of the Kashmir intermontane basin, northwestern Himalaya. *PPP*. 1983 **43(3-4):**205-35.

Census of India 2011 *Provisional Population Totals*. Web : http://censusindia.gov.in/
Cohen, A.C., 1991, Truncated and censored samples—theory and application: New York, Marcel-Dekker, 312 p.

Cohn, T.A., England, J.F., Berenbrock, C.E., Mason, R.R., Stedinger, J.R., Lamontagne, J.R., 2013. A generalized Grubbs-Beck test statistic for detecting multiple potentially influential low outliers in flood series. Water Resour. Res. 49, 5047–5058. doi:10.1002/wrcr.20392

Cohn, T.A., Lane, W.L., Baier, W.G., 1997. An algorithm for computing moments-based flood quantile estimates when historical flood information is available. Water Resour. Res. 33, 2089–2096.

Cohn, T.A., Lane, W.L., Stedinger, J.R., 2001. Confidence intervals for Expected Moments Agorithm flood quantiles estimates. Water Resour. Res. 37, 1695–1706.

Cunderlik, J.M., Burn, D.H., 2003. Non-stationary pooled flood frequency analysis. J. Hydrol. 276, 210–223. doi:10.1016/S0022-1694(03)00062-3

Das, M.R., Mukhopadhyay, R.K., Dandekar, M.M., Kshirsagar, S.R. 2002. Pre-monsoon western disturbance in relation to monsoon rainfall, its advancement over NW India and their trends. *Current Sc*i. **82(11)**, 1320–1321.

Digby, W. 1890. *Condemned Unheard, India and Kashmir*. London.

Eddy, J.A. 1976. The maunder minimum. *Science*, ***192*****(4245)**:1189-1202.

Ely, L.L., Enzel, Y., Baker, V.R., Kale, V.S., Mishra, S. 1996. Changes in the magnitude and frequency of late Holocene monsoon floods on the Narmada River, central India. *Geol Soc Am Bull*, **108(9):** 1134-1148.

England, J.F., Cohn, T.A., Faber, B.A., Stedinger, J.R., Thomas, W.O., Veilleux, A.G., Kiang, J.E., Mason, R.R., 2018. Guidelines for Determining Flood Flow Frequency−Bulletin 17C (ver. 1.1, May 2019). U.S. Geological Survey Techniques and Methods, book 4, chap. B5, Reston, Virginia. doi:10.3133/tm4B5

England, J.F., Salas, J.D., Jarrett, R.D., 2003. Comparisons of two moments-based estimators that utilize historical and paleoflood data for the log Pearson type III distribution. Water Resour. Res. 39. doi:10.1029/2002WR001791

Farooq, M. 2014 *A Satellite based rapid assessment on flood in Jammu and Kashmir – September 2014* (Department of Environment and Remote Sensing. Govt. of Jammu and Kashmir, Srinagar)

Govindha Raj, K. B. 2010) Remote sensing based hazard assessment of glacial lakes: a case study in Zanskar basin, Jammu and Kashmir, India. *Geomat Nat Haz Risk* **1(4):** 339-347.

Gosain, A.K., Rao, S., Basuray, D. 2006. Climate change impact assessment on hydrology of Indian river basins. *Curr sci* **90(3)**: 346-353

IWT 1960. *Indus Waters Treaty between the Government of India and the Government of Pakistan*, signed at Karachi, on 19 September 1960 (entered into force 1 April 1960).

Jie, W., Vitart. F., Wu, T., Liu, X. 2017. Simulations of the Asian summer monsoon in the sub-seasonal to seasonal prediction project (S2S) database. *Q J Roy Met*, **143(706):** 2282-2295.

Kale, V.S. 1997. Flood studies in India: A brief review. *J. Geo. Soc. India* ***49*****(4)**: 359-370.

Kale, V.S., Baker, V.R. 2006. An extraordinary period of low-magnitude floods coinciding with the Little Ice Age: palaeoflood evidence from Central and Western India. *J. Geol. Soc. India*, **68(3):** 477.

Kale, V.S., Hire, P., Baker, V.R. 1997a Flood hydrology and geomorphology of monsoon-dominated rivers: the Indian Peninsula. *Water Int*. **1**; 22(4):259-65.

Kale, V.S., Hire, PS. 2007. Temporal variations in the specific stream power and total energy expenditure of a monsoonal river: The Tapi River, India. *Geomorphology* **92(3-4)**: 134-146.

Kale, V.S., Singhvi, A.K., Mishra, P.K., Banerjee, D. 2000. Sedimentary records and luminescence chronology of Late Holocene palaeofloods in the Luni River, Thar Desert, northwest India. *Catena* **40(4)**: 337-358.

Kalsi, S.R. 1980 On some aspects of interaction between middle latitude westerlies and monsoon circulation. *Mausam* **38(2)**: 305–308.

Kaul, M.N. 1990. Glacial and Fluvial Geomorphology of Western Himalaya: Liddar Valley. Concept Publishing Company.

Koppen, W. 1936 *Das geographisca System der Klimate*, Borntraeger, 1–44.

Kumar, R., Acharya, P. 2016 Flood hazard and risk assessment of 2014 floods in Kashmir Valley: a space-based multisensor approach. *Nat. Hazards* **84**: 437–464.

Kundzewicz, Z.W., Graczyk, D., Maurer, T., Pińskwar, I., Radziejewski, M., Svensson, C., Szwed, M., 2005. Trend detection in river flow series: 1. Annual maximum flow. Hydrol. Sci. J. 50, 797–810. doi:10.1623/hysj.2005.50.5.797

Lang, M., Ouarda, T.B.M.J., Bobée, B. 1999. Towards operational guidelines for over-threshold modeling. *J Hydro* **225**: 103–117

Lawrence, W.R. 1895. *The Valley of Kashmir (Reprinted)*. Srinagar: Chinar Publishing House.

Malik, M.I., Bhat, M.S. 2014. Integrated approach for prioritizing watersheds for management: A study of lidder catchment of kashmir himalayas. *Environ Manag*. **54(6)**: 1267-1287.

Meraj, G., Romshoo, S.A., Yousuf, A.R., Altaf, S., Altaf, F. 2015. Assessing the influence of watershed characteristics on the flood vulnerability of Jhelum basin in Kashmir Himalaya. *Nat Hazards* **77(1)**: 153-175.

Murakami, H., Vecchi, G.A., Underwood, S. 2017. Increasing frequency of extremel severe cyclonic storms over the Arabian Sea. *Nat Clim Change* **7(12)**: 885

Naulet, R., Lang, M., Ouarda, T.B., Coeur, D., Bobée, B., Recking, A., Moussay, D. 2005. Flood frequency analysis on the Ardèche river using French documentary sources from the last two centuries. *J Hydro*, **313(1-2)**: 58-78.

Palazzi, E., Von Hardenberg, J., Provenzale, A. 2013. Precipitation in the Hindu-Kush Karakoram Himalaya: observations and future scenarios. *J Geophys Res Atmos*, **118(1)**: 85-100.

Pepin, N., Bradley, R.S., Diaz, H.F., Baraër, M., et al., 2015 Elevation-dependent warming in mountain regions of the world. *Nat Clim Change* **5(5)**: 424.

Rajatarangini Kalhanas, 1149. Translated by Dutt (1879) *Kings of Káshmír: Being a Translation of the Sanskrita Work Rájataranggini of Kahlana Pandita*.

Rao, F.A. 2018. *Water, polity and Kashmir*. Institute of Public Policy, Research and Development. Gulshan, Srinagar.

Rao, K.K., Patwardhan, S.K., Kulkarni, A., Kamala, K., Sabade, S.S., Kumar, K.K. 2014. Projected changes in mean and extreme precipitation indices over India using PRECIS. *Glob Planet Change* **113**: 77-90.

Rashid, I., Bhat, M.A., Romshoo, S.A. 2017. Assessing changes in the above ground biomass and carbon stocks of Lidder valley, Kashmir Himalaya, India. *Geocarto int*. **32(7)**: 717-734.

Rashid, I., Romshoo, S.A., Chaturvedi, R.K., Ravindranath, N.H., Sukumar, R., et al., 2015. Projected climate change impacts on vegetation distribution over Kashmir Himalayas. *Clim. Change* **132(4)**: 601-613.

Rather, M.I., Rashid, I., Shahi, N., Murtaza, K.O., et al., 2016 Massive land system changes impact water quality of the Jhelum River in Kashmir Himalaya. *Environ Monit Assess* **188(3)**: 185.

Ray, K., Bhan, S.C., Bandopadhyay, B.K. 2015 The catastrophe over Jammu and Kashmir in September 2014: a meteorological observational analysis. *Curr Sci*. 580-591.

Reddy, C.S., Jha, C.S., Dadhwal, V.K., et al., 2016 Quantification and monitoring of deforestation in India over eight decades (1930–2013). *Bio Cons* **25(1)**: 93-116.

Romshoo, S.A., Altaf, S., Rashid, I., Dar, R.A. 2018 Climatic, geomorphic and anthropogenic drivers of the 2014 extreme flooding in the Jhelum basin of Kashmir, India. *Geo. Nat. Hazards & Risk* **9(1)**: 224-248.

Rowan, A.V., 2017. The 'Little Ice Age'in the Himalaya: A review of glacier advance driven by Northern Hemisphere temperature change. *The Holocene*, ***27*(2) :** 292-308.

Salas, J.D., 1993. Analysis and modeling of hydrologic time series, in: Maidment, D.R. (Ed.), Handbook of Hydrology. McGraw-Hill, New York, pp. 19.1-19.72.

Shindell, D.T., Schmidt, G.A., Mann, M.E., Rind, D., Waple, A. 2001. Solar forcing of regional climate change during the Maunder Minimum. *Science*, **294(5549)**: 2149-2152.

Stedinger, J.R., Cohn, T., 1986. Flood frequency analysis with historical and paleoflood information. Water Resour. Res. 22 (5), 785–793.

Tabish, S.A., Nabia, S. 2015. Epic tragedy: Jammu & Kashmir floods: a clarion call. *Emerg. Med.* **5(233):** 2

Thomas, P.J., Juyal, N., Kale, V.S., Singhvi, A.K. 2007. Luminescence chronology of late Holocene extreme hydrological events in the upper Penner River basin, South India. *J Quat Sci.* **22(8):** 747-753.

Treydte, K.S., Schleser, G.H., Helle, G., Frank, D.C., Winiger, M., Haug, G.H., Esper, J. (2006) The twentieth century was the wettest period in northern Pakistan over the past millennium. *Nature*. **440**(7088):1179.

Turner, A.G. Annamalai, H. 2012. Climate change and the South Asian summer monsoon. *Nat. Clim. Chan.* ***2*(8)**: 587.

Venugopal, R., Yasir, S., 2017. The politics of natural disasters in protracted conflict : the 2014 flood in Kashmir. *Oxford Dev. Stud.* **45.4**: 424-442.

Wani, A.A., Joshi, P.K., Singh, O., Shafi, S. 2016. Multi-temporal forest cover dynamics in Kashmir Himalayan region for assessing deforestation and forest degradation in the context of REDD+ policy. *J Mt Sci* **13(8)**: 1431-1441.

Wasson, R.J., Sundriyal, Y.P., Chaudhary, S., Jaiswal, M.K., Morthekai, P., Sati, S.P., Juyal, N. 2013. A 1000-year history of large floods in the Upper Ganga catchment, central Himalaya, India. *Quaternary Sci Rev* **77**: 156-166.

Webster, P.J., Toma, V.E., Kim, H.M. 2011. Were the 2010 Pakistan floods predictable?. *Geophys. Res. Lett.*, **38(4).**

Wilhelm, B., Ballesteros Cánovas, J.A., Macdonald, N., Toonen, W.H., et al., (2019). Interpreting historical, botanical, and geological evidence to aid preparations for future floods. *Water* **6(1)**: e1318